Correlating In silico Feed-forward Loop Knockout Experiments with the Topological Features of Transcriptional Regulatory Networks

Ahmed F. Abdelzaher [*] Michael L. Mayo [†] Edward J. Perkins

Preetam Ghosh

ABSTRACT

Motifs and degree distribution in transcriptional regulatory networks play an important role towards their fault-tolerance and efficient information transport. In this paper, we designed an innovative in silico feed-forward loop motif knockout experiment to assess their impact on the following six topological features: average shortest path, diameter, closeness centrality, betweenness centrality, global and local clustering coefficients. The experiments were conducted on the transcriptional regulatory network of E. coli. The purpose of this study is two-fold: (i) motivate the design of more accurate transcriptional network growing algorithms that can produce similar degree and motif distributions as observed in real biological networks and (ii) design more efficient bio-inspired wireless sensor network topologies that can inherit the robust information transport properties of biological networks.

Categories and Subject Descriptors

J.3 [**Medical Information Systems**]; C.2.1 [**Network Architecture and Design**]

General Terms

Theory; Algorithms

[*]A. Abdelzaher (abdelzaheraf@vcu.edu) and P. Ghosh (pghosh@vcu.edu) are with the Virginia Commonwealth University, School of Engineering Department of Computer Science. Address: 801 W. Main St. Richmond, VA 232084.

[†]M. L. Mayo (Michael.L.Mayo@usace.army.mil) and E. J. Perkins (Edward.J.Perkins@usace.army.mil) are with the Environmental Laboratory, US Army Engineering Research and Development Center, Vicksburg, MS 39180.

BICT 2014, December 01-03, Boston, United States

DOI 10.4108/icst.bict.2014.257916

Keywords

Shortest path; Centrality; Graph Randomization; Clustering Coefficient; Feed-forward loop

1. INTRODUCTION

The ability for networks to rewire it's links was introduced by biologists when they realized that biological networks can resist external perturbations, yet proceed with their natural activities. This property was referred to as 'Biological Robustness' [25], and was mainly attributed to these network's topological features [26]. For example in the proposed bio-inspired self organizing wireless sensor and actuator network [4], edge rewiring must guarantee optimal topological preservation in case of nodal collapse.

Among the features that aid in network dynamics, is the fact that biological networks are sparse [16], or loosely connected. In such networks, degree distributions can be expressed using a power law, $p(k) \sim k^{-\gamma}$ [7], meaning, a steep negative slope will result from the bi-log plot of the different nodal degrees vs. the nodes that have such degrees. Consequently, few nodes have degrees much higher than the average degree (i.e hubs) [5], while the bulk of the remaining nodes have degrees much lower than the average, resulting in loosely connected components. For example, most gene nodes in the transcriptional network of Escherichia coli (herein E. coli), have single incoming reactions and no outgoing ones.

Most biological networks have $2 < \gamma < 3$ [7]- a property which classifies a network as 'scale-free' [5]. The significance of networks having hub to low degree orientations, can be expressed through the reduced probability of having a detrimental random attack. Most random attacks will result in loss of minimal links [8]. Similarly with edge rewiring, the relative overall damage to the entire network will not be too high. However intentional hub attacks can be very costly and can result in disconnecting the network [9].

Other network classifications fall under two other major categories, namely random(ER) [12] and small-world(SW) [42] networks. The preceding considers links

connecting two nodes at equal probabilities during growth, while the latter is inclined towards minimizing the number of hops between pairs of nodes. In contrast with scale-free networks, systems grow using 'the rich get richer and the poor get poorer' phenomena. ER and SW networks typically have tightly connected components, which is different from that of scale-free networks. Nodal degrees is almost equal to the average degree, therefore making random attacks as equally costly as intentional attacks [5].

Another important aspect that aids in biological robustness, is the existence of $3-6$ nodal substructures known as 'motifs' [28]. For example, ecologists believe that synthetic communities forming motifs can be inserted with weak interactions to increase the community's stability [37]. These substructures are labeled 'significant' because their numbers in the real networks are much higher as compared with their numbers in multiple randomized versions of these networks [28, 32]. Moreover, we will show in this paper that motif abundance aids the overall information transport in such transcriptional regulatory networks (herein TRN).

Understanding the underlying architecture of TRNs can provide insights in disease dynamics and drug development [13, 29]. In a TRN, nodes portray the genes in a cell, and a set of directed links that correspond to interacting pairs or genes [40]. Interactions could either represent translation or transcription [14]. Unlike engineered networks, TRNs exhibit biological robustness [25, 26] due to their tolerance of noise during gene expression [35]. This phenomena arises from feed-back control nodal arrangements and repetitive substructures [35], or motifs.

Among the significant 3-node motifs in TRNs, the feed-forward loop (or FFL) has received the most attention. An FFL consists of a transcription factor A that regulates another transcription factor B and a gene C, while B co-regulates C. This topology allows it to deliver essential tasks like generating pulses, irreversible speed ups and signal delays [39].

At the nodal level, research has been directed towards assessing robustness correlation with disturbances in the network. For example the effect of nodal collapse has been modeled to show a decrease in network efficiency [15, 10]- which is defined as the inverse of the average shortest path in the network. Successive random nodal deletions have been plot against network diameter for scale-free and ER networks [5, 8]. Others model disturbances in the form of connection failures [11], or partial inactivation [3], where the length of the links in the TRN of E. coli were increased to resemble interaction delays.

At the motif level, much attention has been focused towards understanding motif functions. Different motif configurations have been investigated using mathematical models of transcription and translation to understand the relationship between coupling and function of embedded motifs [24, 23]. Experiments with E. coli have been conducted were transcription factors were rewired and the tolerance of the bacteria was analyzed [19].

However, little is known regarding the motif distribution in the network and it's contributions towards robustness, particularly in terms of information transport. We address this issue with successive in silico FFL knock-outs in E. coli, while preserving the individual in-, out- and cumulative degrees of the nodes. After every successive FFL deletion, different topological metrics were recorded. Then, Pearson's correlation coefficient is used to determine the correlation between each pair of metrics studied here.

2. MOTIVATION

2.1 Bio-Inspired Wireless Sensor Networks

Resemblance between gene regulation systems and wireless sensor networks (herein WSNs) can be described through transcription, where genes process signals from adjacent neighbors in the form of transcription factors that excite/repress other genes by generating mRNA molecules. TRN nodes interface through conveying signals (transcription factors), that are then processed into output signals (mRNAs). WSNs operate in a similar manner, where sensor nodes send signals to others in the form of data packets. Packets at destination nodes convey forwarding instructions, which in return relays such packets to other sensors.

Recently, we have shown that WSNs adopting TRN topologies, designated as bio-inspired WSNs, are more efficient than those adopting ER topologies of the same size in terms of conveying packets to sink nodes [21, 20, 17]. A support vector machine model was constructed with $\sim$ 90% accuracy to predict packet receipt rates using the topological features of the networks as input [2, 22] that includes the average degree, network density, as well as the abundance of FFLs. Each of these three topological features were ranked higher than the other ones. It is hence important to study how FFL abundance positively or negatively correlate with the other topological features in the network. Such a study will motivate the design of smart WSN topologies that exhibit similar FFL abundance as observed in the TRNs of E. coli and hence will have better efficiency in terms of their average packet receipt rates.

2.2 Biological Network Growing Algorithms

Another popular area of research includes the transcriptional network growing algorithms primarily based on the preferential attachment model [6]. Currently, only the TRNs of E. coli and yeast have been validated experimentally; hence such network growing algorithms are essential to allow the community to study the properties of such TRNs, design robust networks, as well as to predict the TRNs of higher-level organisms. We have recently developed such a network growing algorithm by extending the preferential attachment model to produce directed networks that mimic the topological properties of E. coli [31] in terms of their degree distribution and FFL abundance.

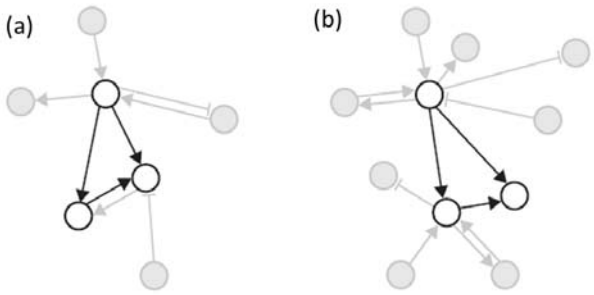

Figure 1: (a) Embedded and (b) Canonical FFLs.

The algorithm adds one foreign node at a time to an existing subgraph of candidate nodes. Based on in- and out-degree centralities of the candidate nodes, attachment kernels are computed [27], which further becomes conditions for foreign nodes attachments. Although this algorithm showed good correspondence in terms of FFL abundance in the predicted networks when compared to the TRN of E. coli, the corresponding distribution of FFLs measured in terms of the number of nodes in the network participating in such FFLs did not match well. Hence, while preferential attachment alone can only produce comparable degree distribution or motif abundance, additional topological metrics must be considered to design more accurate algorithms for growing TRNs. Our work in this paper, is hence important as we identify the topological metrics that strongly correlate with FFLs as observed from successive FFL deletions from the original E. coli TRN.

3. E. COLI TRANSCRIPTIONAL NETWORK

We consider the TRN of E. coli, wherein $\gamma = 2.1 \pm 0.3$ [41]. The TRN was rendered using GeneNetWeaver [38]- a bioinformatics software tool which was originally designed to asses the accuracy of reverse engineered GRNs of E. coli and Yeast. E. coli is composed of 1565 nodes and 3758 interconnections, together forming 23 disjoint components.

A TRN is represented using a square matrix T. A direct connection originating from node i incident on node j in a TRN is represented by cell $T_{ij} = 1$, and the absence of such connection designates $T_{ij} = 0$. Because TRN edges carry no weight, T can only hold values of 0 and 1.

In a TRN of size n, we consider two methods for counting the occurrences of FFLs. The first method considers all available 3 node combinations forming at least one FFL; we designate such FFLs as the "embedded" FFLs. This can be determined computationally using,

$$m_1 = \sum_{i=1}^{n}\sum_{j=1}^{n}\sum_{k=1}^{n}\left[T_{ij} \cap T_{ik} \cap T_{jk}\right], \quad T_{ij} = T_{ik} = T_{jk} = 1. \tag{1}$$

The second method considers all 3 node combinations which form only FFLs and no other 3 node substructure; we designate such FFLs as the "canonical" FFLs. This can be computed using,

$$m_2 = \sum_{i=1}^{n}\sum_{j=1}^{n}\sum_{k=1}^{n}\left[T_{ij} \cap T_{ik} \cap T_{jk}\right], \quad T_{ij} = T_{ik} = T_{jk} = 1, \quad T_{ji} = T_{ki} = T_{kj} = 0. \tag{2}$$

Figure 1 illustrates the two types of FFLs considered in this paper.

4. ANALYSIS ALGORITHM

For simplicity, we designate the initial value of m_1 as $m_{1,0}$ (i.e., at iteration zero) and $m_{1,j}$ denotes the number of embedded FFLs at the j^{th} iteration. The algorithm starts by computing $m_{1,0}$ and the different topological metrics discussed in the next section. Next, the network goes through a predefined number of iterations, wherein at each iteration we make a switch between two edges that involve four distinct nodes following the method proposed in [34]. The switch picks two edges at random, having two random source and destination nodes, s_1, s_2, d_1, and d_2 respectively. Edges are next rewired so that s_1 connects d_2 and s_2 connects d_1.

Every iteration is considered successful if the following two conditions are satisfied:

1. The rewiring of edges should not affect any other existing edge in the network. Doing so, the overall in-, out- and cumulative degree distributions stay exactly the same while the overall topology is altered. Hence, the number of FFLs are changed.

2. For the j^{th} iteration, $m_{1,j} < m_{1,j+1}$ must hold in order to proceed to the next iteration. This guarantees that one or more FFLs were deleted before starting the next iteraiton.

If either of the conditions are not satisfied, the iteration is repeated. This process continues for 200 iterations that was arbitrarily set and was enough to properly identify the correlations and trends that we report here. At each iteration, each of the other topological metrics as discussed next are also computed. The same process is also followed for our experiments with m_2 deletions.

5. TOPOLOGICAL METRICS

Here we report the six topological metrics considered in this paper. Other metrics were either not affected by FFL knock-outs or did not show any interesting properties based on the information transport or edge rewiring capabilities of the E. coli TRN.

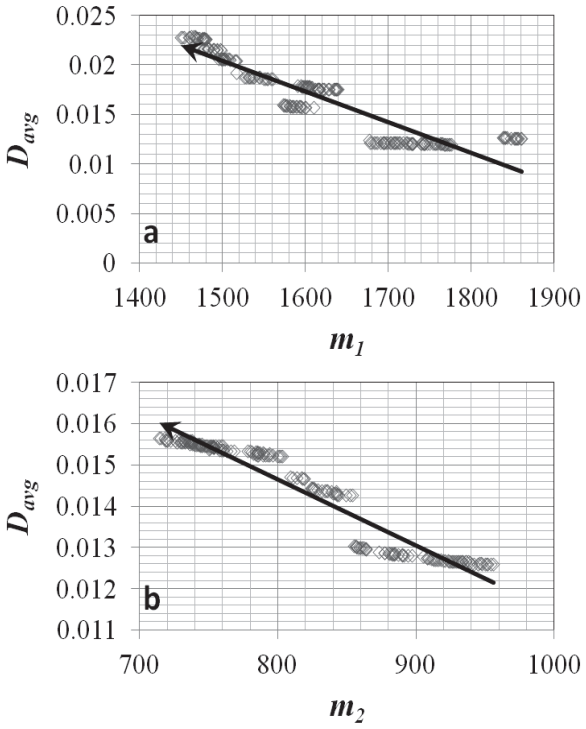

Figure 2: Changes in D_{avg} of E. coli's TRN as a function of the abundance of (a) embedded FFLs and (b) canonical FFLs. The solid arrow shows the direction and the linear trend for the successive values of D_{avg}.

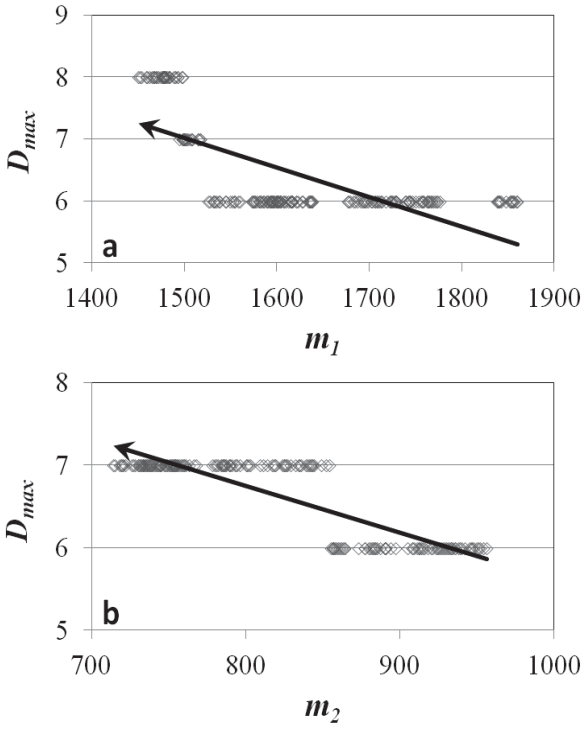

Figure 3: Changes in the diameter of E. coli's TRN as a function of the abundance of (a) embedded FFLs and (b) canonical FFLs.

5.1 Average Shortest Path

The average shortest path measures the average number of hops along the shortest paths between all possible node pairs in the network and is considered as one of the most robust metrics for assessing network efficiency in terms of information transport. We compute D_{avg} using,

$$D_{\text{avg}} = \frac{\sum_{i=1}^{n}\sum_{j=1}^{n} d_{ij}}{n(n-1)}, \quad d_{ij} \neq \infty, \tag{3}$$

where d_{ij} is the shortest path between nodes i and j. $d_{ij} = \infty$ signifies that a path does not exist. Figure 2 plots the successive FFL deletions vs D_{avg} and shows that D_{avg} is negatively correlated with both embedded and canonical FFLs. FFL structures decrease the average number of hops between the nodes in the TRN, and hence, play a major role in it's efficiency.

5.2 Diameter

Although the maximum shortest path D_{max} is known to correlate positively with D_{avg}, and hence negatively with FFL counts, we find D_{max} useful in other means. Since the metric considers the maximum of the paths, it should be more stable to changes in m_1 and m_2. As shown in Figure 3, D_{max} sustained almost 350 m_1 and 125 m_2 deletions before increasing in value. However, the points at which D_{avg} increase are focal points for attention because they can help us pinpoint the more important FFLs.

5.3 Closeness Centrality

The closeness centrality C_i measures the relative closeness of node i to every other node in the network. A close node is capable of delivering information quicker to other nodes [33]. Central nodes in biological networks are crucial because they play the roles of 'organizational hubs' [43]. The closeness centrality of node i, C_i, is computed by,

$$C_i = \frac{n-1}{\sum_{i=1}^{n} d_{ij}}, \quad d_{ij} \neq \infty, \tag{4}$$

having values $[0, 1]$, with 0 meaning i is disconnected from the network, and 1 meaning node i has a direct link to every node.

It is important to note that an increase in C_i signifies an increase in communicative efficiency, however, it is not the case with resilience to random attacks. For example, if all nodes have $C_i = 1$, meaning each node is connected to one another by a direct link. A random attack on any node would cost the network $n-1$ links. For the entire network we compute the average closeness,

$$C_{\text{avg}} = \frac{n-1}{n\sum_{i=1}^{n} d_{ij}}, \quad d_{ij} \neq \infty. \tag{5}$$

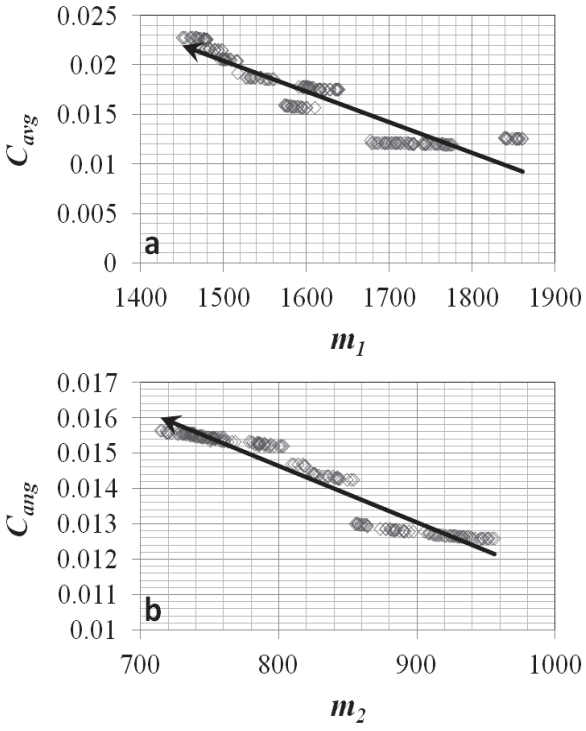

Figure 4: Changes in the C_{avg} of E. coli's TRN as a function of the abundance of (a) embedded FFLs and (b) canonical FFLs.

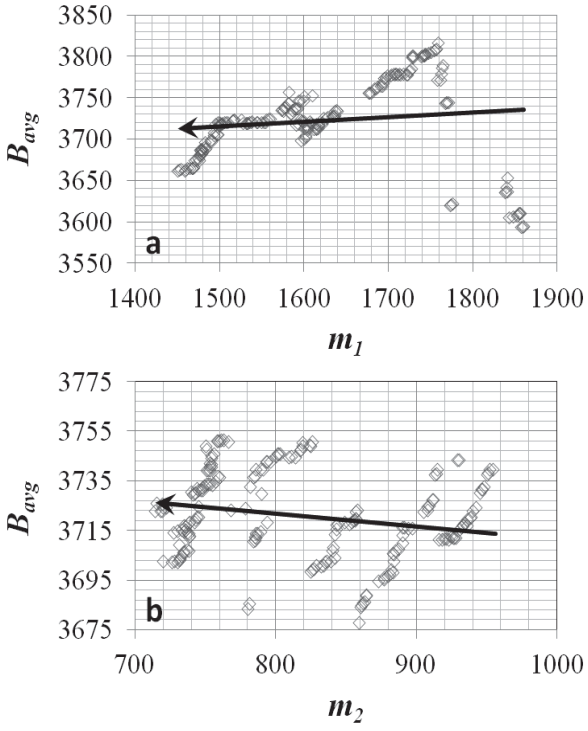

Figure 5: Changes in the B_{avg} of E. coli's TRN as a function of the abundance of (a) embedded FFLs and canonical FFLs.

Figure 4 depicts a negative correlation between the average closeness centrality C_{avg} and the embedded and canonical FFL abundances. FFLs seem to preserve the 'scale-free' property of the network wherein a decrease in FFL counts cause an increase in the average closeness, which further means that the hub node strengths shift to other nodes in the network. The availability of centralized nodes fades as the FFLs are deleted, making the network more communicatively efficient, however, less resilient to random attacks.

5.4 Betweenness Centrality

Betweenness centrality for a node computes the fraction of shortest paths passing through a node divided by the number of all shortest paths in the system. Assuming that information transfer goes along the shortest paths, a node having high betweenness will have a large influence in general. For example, a study of yeast has shown that essential proteins have relatively high betweenness [1].

In order to analyze the whole network, we compute a global average betweenness as follows,

$$B_{\text{avg}} = \frac{1}{n} \sum_{v=1}^{n} \sum_{i=1}^{n} \sum_{j=1}^{n} \frac{\sigma_{ij}(v)}{\sigma_{ij}}, \quad i \neq v \neq j, \tag{6}$$

where σ_{ij} denotes the number of shortest paths between i and j, and $\sigma_{ij}(v)$ is the number of those paths that pass through v. The successive FFL deletion plot in Figure 5 shows a weak correlation with average betweenness values. However, this observation is significant, because betweenness plays a role in forming communities within the network, hence, affects it's robustness. Having no correlation with FFL abundance hence implies that this metric should be considered separately on top of preferential attachment models to predict more accurate TRN topologies.

5.5 Global Clustering Coefficient

Clustering coefficient measures the tendency for a network to form clusters. Evidence shows that real-world networks create denser ties than ER networks [42]. Moreover, robust biological networks having scale-free distributions, exhibit short average paths and high clustering coefficients [18, 36]. We denote the global clustering coefficient by α_1, which is computed by dividing thrice the number of completely connected nodes by the number of triplets (i.e open loops). Figure 6 shows the changes in α_1 by our FFL knockout experiments. Although we observe no correlation with FFLs, as with B_{avg}, this metric will hence need separate consideration in designing better TRN growing algorithms.

5.6 Average Local Clustering Coefficient

An alternative to α_1, is the average local clustering coefficient [42], formally defined as

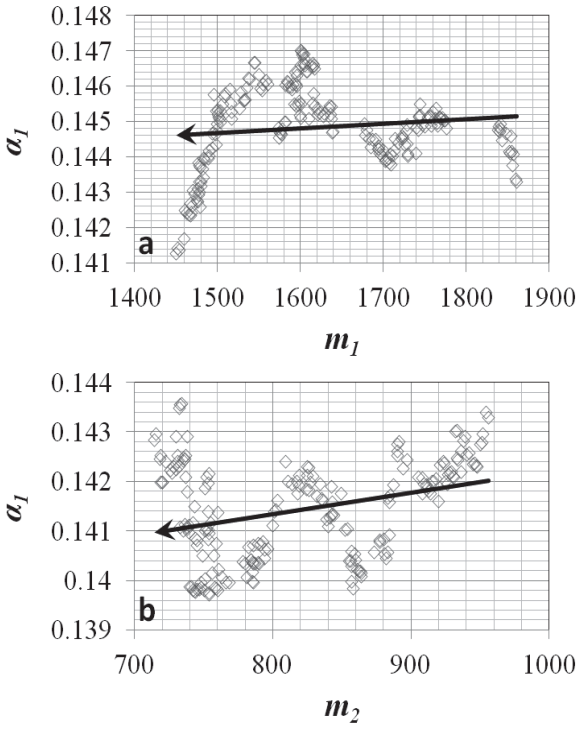

Figure 6: Changes in the α_1 of E. coli's TRN as a function of the abundance of (a) embedded FFLs and (b) canonical FFLs.

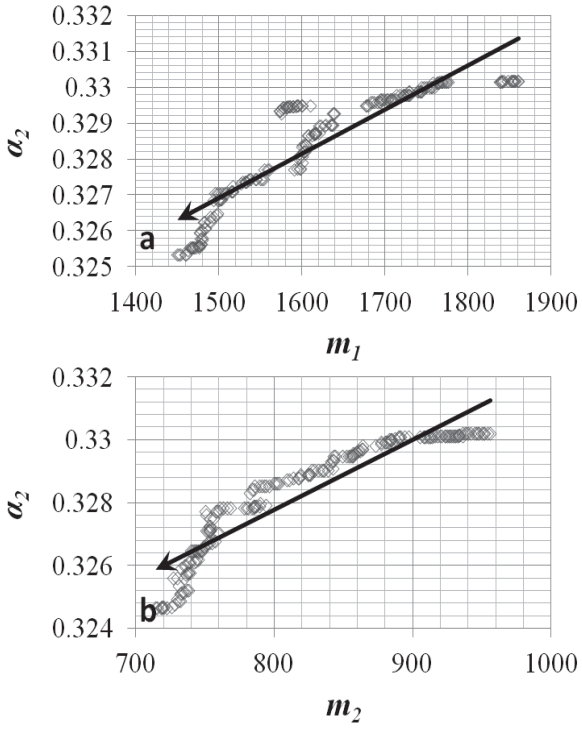

Figure 7: Changes in the α_2 of E. coli's TRN as a function of the abundance of (a) embedded FFLs and (b) canonical FFLs.

$$\alpha_2 = \frac{1}{n}\sum_{i=1}^{n}\frac{\sum_{j=0}^{n} T_{ij}}{k_i(k_i-1)}. \quad (7)$$

k_i denotes the number of neighbours for node i, while the metric measures the number of edges connecting the nodes as a fraction of the number of possible edges that could exist in their local communities. At the individual node level, this metric can be used to quantify relative nodal participation in embedded clusters. Figure 7 shows a positive correlation with both embedded and canonical FFLs, meaning there is a decrease in the number of local communities as FFLs get deleted. This supports the observation stated by [18, 36] that scale-free networks typically tend to form clusters.

6. CORRELATION BETWEEN THE TOPOLOGICAL FEATURES

As our primary goal was to study the impact of FFLs on the six different topological features in TRNs, we reported the correlation of FFL abundance to each of these metrics above. However, our FFL knock-out experiments also allows us to compute the pair-wise correlation between these six metrics and FFL abundance using a 7×7 correlation matrix. This correlation matrix was computed using Pearson's correlation coefficient where the values range from -1 to 1, with 1 showing perfect positive correlation, -1 showing perfect negative dependency, and 0 meaning completely independent of one another. A Matlab module [30], colormap(gray) was then used to illustrate the gray scale matrix of the correlation coefficients in Figure 8. Colors closer to black correspond to almost -1 correlation, and white for 1.

The figure summarizes the impact of embedded and canonical FFLs on the other 6 topological features (first column in the correlation matrix). We observe a strong positive correlation with the average global and local clustering coefficient and strong negative correlation with average shortest path and average closeness centrality metrics. While the preferential attachment model for TRN growth algorithms conceptually guarantees high local clustering coefficients, it does not inherently impact the average shortest path or average closeness centrality. So, should one consider both of these metrics in addition to preferential attachment to design new TRN growth algorithms? The correlation matrix however shows a strong positive correlation between average shortest path and closeness centralities suggesting that consideration of any one of these two metrics will be sufficient.

Similarly, average betweenness centrality is not correlated with FFLs in the network and needs to be considered separately. Interestingly, betweenness centrality seem to be independent of all the other features that we have considered here, meaning that the average betweenness central-

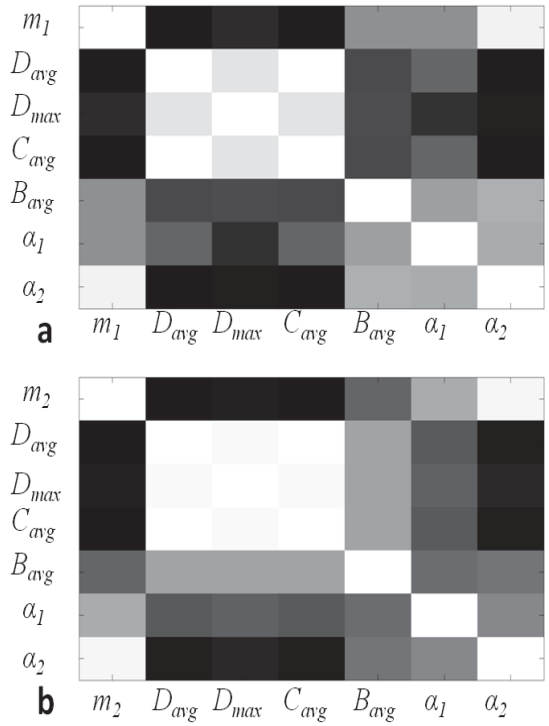

Figure 8: Gray-scale Pearson correlation matrix between the six topological features and (a) embedded and (b) canonical FFLs.

ity must be checked separately when adding each node to the substrate network using the preferential attachment model. Only node additions resulting in an increase of the betweenness centrality values should be allowed.

7. CONCLUSIONS

In this paper, we designed an innovative feed-forward loop motif knockout experiment to assess the impact of such FFL deletions on other topological metrics in the TRN of E. coli. The purpose of this study is two-fold: motivate the design of more accurate TRN growing algorithms as well as design more efficient bio-inspired wireless sensor network topologies. While similar characteristics were observed for embedded and canonical FFLs, it turns out that average betweenness centrality is an important metric to consider on top of preferential attachment models to design such network topologies. Also, FFL knockouts show strong negative correlation with average shortest path and average closeness centrality. As these two metrics are related and contribute to lower end to end delays for information transport, such negative correlation indirectly illustrate the importance of FFLs in facilitating the information transport in such networks.

8. ACKNOWLEDGMENTS

Funding was provided by the US Army's Environmental Quality and Installation 6.1 Basic Research program. The Chief of Engineers approved this material for publication.

9. REFERENCES

[1] *J Biomed Biotechnol*, 30:96–103, June 2005.

[2] A. Abdelzaher, B. K. Kamapantula, P. Ghosh, and S. K. Das. Empirical prediction of packet transmission efficiency in bio-inspired wireless sensor networks. In A. Abraham, A. Y. Zomaya, S. Ventura, R. Yager, V. SnÃąsel, A. K. Muda, and P. Samuel, editors, *ISDA*, pages 705–710. IEEE, 2012.

[3] V. Agoston, P. Csermely, and S. Pongor. Multiple weak hits confuse complex systems: a transcriptional regulatory network as an example. *Phys Rev E Stat Nonlin Soft Matter Phys.*, May 2005.

[4] I. F. Akyildiz and I. H. Kasimoglu. Wireless sensor and actor networks: research challenges. *Ad Hoc Networks*, 2(4):351–367, 2004.

[5] R. Albert, H. Jeong, and A.-L. Barabási. Error and attack tolerance of complex networks. *Nature 406*, pages 378–382, July 2000.

[6] A.-L. Barabasi and R. Albert. Emergence of scaling in random networks. *Science*, 286(5439):509–512, 1999.

[7] A. Clauset, C. R. Shalizi, and M. E. J. Newman. Power-law distributions in empirical data. *SIAM Review*, 51(4):661–703, 2009.

[8] R. Cohen, K. Erez, D. ben Avraham, and S. Havlin. Resilience of the internet to random breakdowns. *Phys. Rev. Lett.*, 85:4626–4628, Nov 2000.

[9] R. Cohen, K. Erez, D. ben Avraham, and S. Havlin. Breakdown of the internet under intentional attack. *Phys. Rev. Lett.*, 86:3682–3685, Apr 2001.

[10] P. Crucittia, V. Latorab, M. Marchioric, and A. Rapisardab. Error and attack tolerance of complex networks. *Physica A: Statistical Mechanics and its Applications*, 340:388–394, 2004.

[11] J. Efstathiou and A. K. Ng. Structural robustness of complex networks. *Proceedings of International Workshop and Conference on Network Science, NetSci 2006*, May 2006.

[12] P. Erdös and A. Rényi. On the evolution of random graphs. *Publ. Math. Inst. Hung. Acad. Sci. 5*, 1960.

[13] J. J. Faith, B. Hayete, J. T. Thaden, I. Mogno, J. Wierzbowski, G. Cottarel, S. Kasif, J. J. Collins, and T. S. Gardner. Large-scale mapping and validation of escherichia coli transcriptional regulation from a compendium of expression profiles. *PLoS biology*, 5(1):e8, 2007.

[14] J. Feng, J. Jost, and M. Qian. *Networks: from biology to theory*. Springer, 2007.

[15] T. Feyessa and M. Bikdash. Measuring nodal contribution to global network robustness. In *Southeastcon, 2011 Proceedings of IEEE*, pages 131 –135, march 2011.

[16] C. Genio, T. Gross, and K. E. Bassler. All scale-free networks are sparse. *Phys Rev Lett*, 107, 2011.

[17] P. Ghosh, M. Mayo, V. Chaitankar, T. Habib, E. Perkins, and S. Das. Principles of genomic robustness inspire fault-tolerant wsn topologies: A network science based case study. *PerCom*

Workshops, pages 160–165, 2011.

[18] K.-. Goh, B. Kahng, and D. Kim. Graph theoretic analysis of protein interaction networks of eukaryotes. *Physica A: Statistical Mechanics and its Applications*, 357(3):501–512, 2005.

[19] M. Isalan, C. Lemerle, K. Michalodimitrakis, C. Horn, P. Beltrao, E. Raineri, M. Garriga-Canut, and L. Serrano. Evolvability and hierarchy in rewired bacterial gene networks. *Nature*, 452(7189):840–5, Apr. 2008.

[20] B. Kamapantula, A. Abdelzaher, P. Ghosh, M. Mayo, E. Perkins, and S. Das. Performance of wireless sensor topologies inspired by e. coli genetic networks. *PerCom Workshops*, pages 302–307, 2012.

[21] B. Kamapantula, A. Abdelzaher, P. Ghosh, M. Mayo, E. Perkins, and S. Das. Leveraging the robustness of genetic networks: a case study on bio-inspired wireless sensor network topologies. *Journal of Ambient Intelligence and Humanized Computing*, 5(3):323–339, 2014.

[22] B. Kamapantula, A. Abdelzaher, M. Mayo, E. Perkins, S. Das, and P. Ghosh. Quantifying robustness in biological networks using ns-2. *Springer-Nanocom*, 2014.

[23] Y. keun Kwon and K. hyun Cho. Boolean dynamics of biological networks with multiple coupled feedback loops, 2007.

[24] J.-R. Kim, Y. Yoon, and K.-H. Cho. Coupled feedback loops form dynamic motifs of cellular networks. *Biophysical Journal*, 94:359–365, January 2008.

[25] H. Kitano. Biological robustness. *Nat Rev Genet*, pages 826–837, November 2004.

[26] H. Kitano. Towards a theory of biological robustness. *Mol Syst Biol 3*, (137), September 2007.

[27] P. L. Krapivsky, S. Redner, and F. Leyvraz. Connectivity of Growing Random Networks. *Physical Review Letters*, 85(21):4629–4632, Nov. 2000.

[28] S. Magnan and U. Alon. Structure and function of the feed-forward loop network motif. *Proc. Natl. Acad. Sci. USA*, October 2003.

[29] A. A. Margolin, I. Nemenman, K. Basso, C. Wiggins, G. Stolovitzky, R. D. Favera, and A. Califano. Aracne: an algorithm for the reconstruction of gene regulatory networks in a mammalian cellular context. *BMC bioinformatics*, 7(Suppl 1):S7, 2006.

[30] MATLAB. *version 7.10.0 (R2010a)*. The MathWorks Inc., Natick, Massachusetts, 2010.

[31] M. Mayo, A. F. Abdelzaher, E. J. Perkins, and P. Ghosh. Motif participation by genes in e. coli transcriptional networks. *Front Physiol*, 3:357, 2012.

[32] R. Milo, S. Shen-Orr, S. Itzkovitz, N. Kashtan, D. Chklovskii, and U. Alon. Network motifs: Simple building blocks of complex networks. *Science 25*, 298(5594):824–827, October 2002.

[33] M. E. J. Newman. A measure of betweenness centrality based on random walks. *Social Networks*, 2005.

[34] M. E. J. Newman, S. H. Strogatz, and D. J. Watts. Random graphs with arbitrary degree distributions and their applications. *Phys. Rev. E*, 64:026118, Jul 2001.

[35] R. J. Prill, P. A. Iglesias, and A. Levchenko. Dynamic properties of network motifs contribute to biological network organization. *PLoS Biol.*, November 2005.

[36] E. Ravasz, A. L. Somera, D. A. Mongru, Z. N. Oltvai, and A. L. Barabási. Hierarchical organization of modularity in metabolic networks. *Science (New York, N.Y.)*, 297(5586):1551–1555, Aug. 2002.

[37] J. M. Rip, K. S. McCann, D. H. Lynn, and S. Fawcett. An experimental test of a fundamental food web motif. *Proc. Biol Sci*, June 2010.

[38] T. Schaffter, D. Marbach, and D. Floreano. Genenetweaver: in silico benchmark generation and performance profiling of network inference methods. *Bioinformatics*, 27(5):2263–70, 2011 Aug 15.

[39] S. S. Shen-Orr, R. Milo, S. Mangan, and U. Alon. Network motifs in the transcriptional regulation network of escherichia coli. *Nature Genetics*, 31:1061–4036, 2002.

[40] I. Shmulevich and E. R. Dougherty. *Probabilistic Boolean Networks – The Modeling and Control of Gene Regulatory Networks*. SIAM, 2010.

[41] A. Vazquez, R. Dobrin, D. Sergi, J. P. Eckmann, Z. N. Oltvai, and A. L. Barabasi. The topological relationship between the large-scale attributes and local interaction patterns of complex networks. *Proc Natl Acad Sci U S A*, 101(52):17940–5+, 2004.

[42] D. J. Watts and S. H. Strogatz. Collective dynamics of 'small-world' networks. *Nature 393*, pages 440–442, June 1998.

[43] S. Wuchty and P. F. Stadler. Centers of complex networks. *J Theor Biol.*, 7:45–53, July 2003.